JOURNAL OF MATERIALS SCIENCE 33 (1998) 2745–2750

Monitoring local strains in cracked cross-ply composites using an embedded aramid fibre strain sensor

B. P. ARJYAL, C. GALIOTIS
Materials Department, Queen Mary & Westfield College, University of London, Mile End Road, London E1 4NS

S. L. OGIN, R. D. WHATTINGHAM
Materials Science & Engineering, University of Surrey, Guildford, Surrey GU2 5XH

Single aramid fibre strain sensors have been embedded in transparent glass-fibre reinforced epoxy resin cross-ply laminates. The sensors, located at the 0°/90°/0° ply interfaces, were interrogated by a remote laser Raman microprobe which enabled the changes in the longitudinal strain in the 0° plies caused by transverse cracking in the 90° ply to be monitored. Strain magnifications of up to about 6 were measured in the crack plane, 10 μm from the 0°/90° ply interface, and it is estimated that the region of enhanced strain extends to a distance of about 40 μm from the interface. Crack interactions were seen to occur for crack spacings of less than two transverse ply thicknesses. © *1998 Kluwer Academic Publishers*

1. Introduction

1.1. Matrix cracking in cross-ply composite laminates

Multiple cracking is a distinctive feature of many types of composite materials. In composite laminates, the prediction of first ply failure, the subsequent accumulation of matrix cracks and consequent mechanical property changes have been the focus of much work over the past twenty years. Transparent cross-ply glass-fibre reinforced epoxy resin (GFRP) laminates have been used in a number of these studies [1, 2] since they show cracking behaviour which is generic for all types of fibre-reinforced plastics and have the added benefit that the damage is easy to observe. Experimental parameters which relate to the macroscopic consequences of matrix cracking and can be measured readily include crack accumulation with increasing stress (or strain) and the resulting laminate changes in stiffness [3], Poisson's ratio [4], coefficient of thermal expansion [5] and residual strain [6]. The theoretical analyses of matrix cracking phenomena which relate to these experimental measurements vary in sophistication: shear-lag analyses [7, 8], more rigorous elasticity analysis [9], variational mechanics [10] and finite element solutions [11] are all available. Each of these approaches varies in the way in which the stress transfer between plies in the vicinity of a matrix crack is treated and it would be valuable, therefore, to have a technique which is able to probe directly local stresses in the laminate.

1.2. Application of laser Raman spectroscopy to fibrous composites

Non-destructive stress or strain measurements in composites can be made by employing the technique of laser Raman spectroscopy [12]. This technique is based on the stress (strain) sensitivity of most Raman vibrational modes of crystalline fibres and is a direct consequence of the change in the bond stiffness with bond extension or contraction [12, 13]. The procedure for stress/strain measurements involves the production of suitable calibration curves in air, which relate the atomic vibrational wavenumbers (frequencies) of reinforcing fibres, such as Kevlar or carbon, to applied values of stress or strain. Hence, the Raman wavenumbers of the embedded fibres in a composite can be converted by means of the calibration curves to values of stress or strain [12, 13]. The superiority of the Raman sensor over other existing sensors is its ability to provide a spatial resolution of 1 μm in measurements of stress or strain. Although this technique has a universal applicability [12], certain amorphous fibres, such as glass, have a very weak Raman response and, therefore, cannot be readily used as intrinsic stress/strain sensors. In order to overcome this problem, a small amount of aramid fibres which exhibit very strong Raman response [14] can be placed at strategic positions within a glass fibre laminate to act as stress or strain Raman sensors. In addition, by matching the refractive index of the polymer matrix to that of the reinforcing fibre (glass), transparent composites can be made, which allow the

interrogation of the aramid fibre at any required depth.

In this work we are studying in detail the matrix cracking phenomenon in glass fibre composites by embedding single aramid stress sensors at the 0°/90° ply interfaces of cross-ply laminates. The aim is to monitor the strains in the 0° ply as a result of matrix cracking in the 90° ply. In a subsequent paper we shall be comparing the results obtained by this technique with existing analytical models.

2. Experimental

2.1. Fabrication of the composite specimens

The transparent cross-ply laminates containing the Kevlar fibres were manufactured using a modified frame-winding technique. Glass fibres were first wound onto an open steel frame, 300 mm square, to form the 90° ply. The individual Kevlar fibres to be used as the strain sensors were extracted carefully from a bundle of Kevlar fibres. To locate the Kevlar fibres at the 0/90 interface and parallel to the 0° fibres, two thin grooved metal cross-pieces were glued to the frame parallel to the 90° fibres and about 240 mm apart. The grooves allowed the accurate location of the Kevlar fibres at a spacing of about 24 mm and parallel to the 0° direction. These fibres were held in place with the aid of silicone rubber which sets to hold the fibres in position, but allows some flexibility so that the fibres do not break where they are held. The steel frame could now be positioned so that the 0° glass fibres were wound over both the 90° glass fibres and the individual Kevlar fibres. Before winding the 0° fibres, two tows of glass fibres were fixed perpendicular to the Kevlar fibres in the grip areas. These two tows, one each near the top and the bottom of the frame, ensured that the Kevlar fibres did not move out of alignment during the overwinding of the 0° fibres and also helped to ensure that the Kevlar fibres did not drift unduly into the 0° tows during winding and curing.

To make a composite panel, the wound fibres were impregnated with the epoxy resin (Shell "Epikote" 828 cured with nadic methyl anhydride and accelerator K61B in the ratio 100:60:4) which was first mixed and degassed before impregnation. Full wetting of the fibres was achieved by placing the uncured laminate inside a vacuum chamber for about 20 min before squeezing out any excess resin and entrapped air bubbles. The laminate was cured between thick glass plates loaded with a 100 kg mass for 3 h at 100 °C, followed by a post-cure at 150 °C for 3 h. The overall dimensions of the panel were 360 mm square, from which coupons 230 mm long by 20 mm wide were cut, each specimen containing a centrally positioned Kevlar fibre (Fig. 1). The final specimens have a transverse ply thickness of 1.22 mm and 0° ply thicknesses of 0.64 mm.

2.2. Remote laser Raman spectroscopy

A novel remote laser Raman microprobe, which has been built and tested recently [15], was used in this

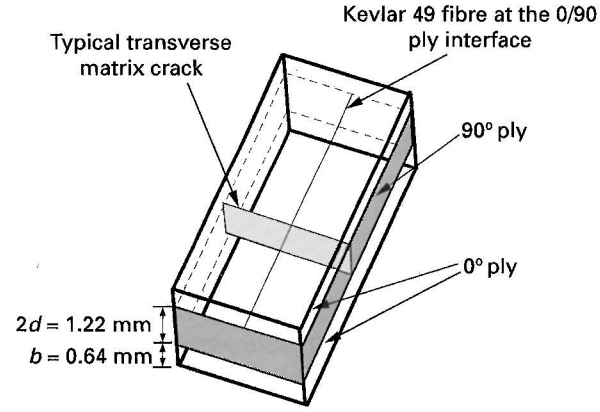

Figure 1 Sketch of a typical $[0/90]_s$ cross-ply composite incorporating a Kevlar 49® filament at one 0/90 interface as an embedded strain sensor. A single transverse crack in the 90° ply is shown.

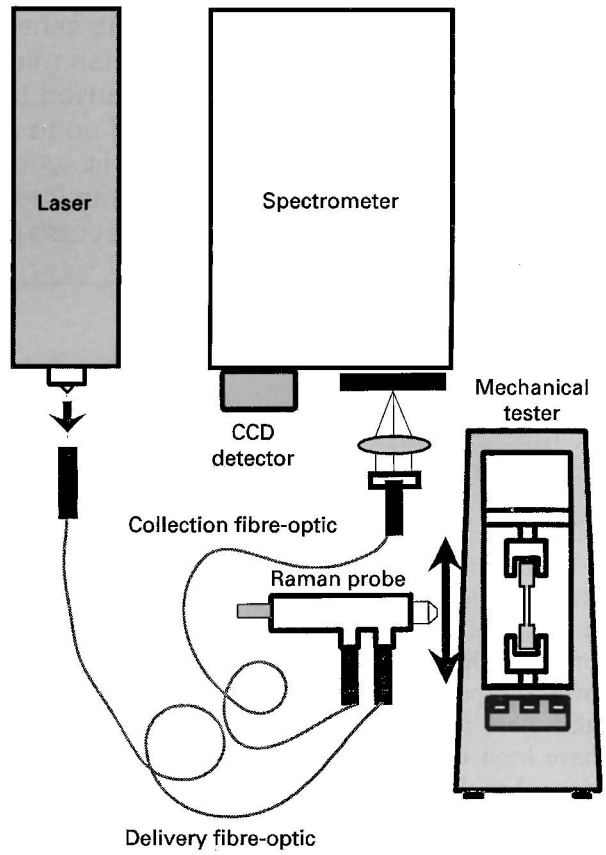

Figure 2 Diagram of the remote laser Raman experimental arrangement.

work. The main feature of the new probe is the use of flexible fibre for laser delivery and collection (Fig. 2), which brings about a complete separation of the spectroscopic and the testing stages. The use of flexible fibre optic cables permits operation of the microprobe in horizontal, vertical and multi-angle positions [15]. Such an arrangement allows the interrogation of specimens of any size and shape under a variety of different environments. In addition, the presence of a miniature CCTV imaging camera on the back of the microprobe allows it to operate simultaneously both as a Raman and an optical microscope. This arrangement is particularly useful for the experiments described here as it

allows measurements on the composite specimens while they are being deformed on the mechanical tester (Fig. 2).

In this work, the source of excitation was the 514.5 nm line of a water-cooled Ar^+ laser. The input laser light was directed on a holographic beamsplitter through a single-mode fibre optic cable (Fig. 2). The light was then focused onto the specimen via a conventional objective (Olympus 50×). The 180° scattered light was collected by the same objective and transmitted through the holographic beamsplitter, which attenuated the 514.5 nm line (Fig. 2). The inelastically scattered light was guided through another optical fibre to a SPEX 1000M single monochromator and was dispersed onto a Wright Instruments air-cooled CCD (charge coupled device). The dispersed Raman signal was then converted to an electrical signal and stored in a PC. The computer software allowed the operator to view the spectra instantly and analyse at a later date. For analysis of spectra, the background was assumed to have a quadratic form and the raw data were fitted with either Lorentzian or Gaussian distributions.

The 1615 cm^{-1} band of a Kevlar 49® fibre, which is primarily attributed to the aromatic ring C–C stretching vibrational mode, has been employed in this work for strain measurements [16]. The raw Raman data for this particular band are best fitted with a Gaussian distribution and a quadratic background [16]. The laser power on the Kevlar 49® fibre was maintained at 0.80 mW to avoid damaging the fibre.

2.3. Mechanical testing

The composites were tested in tension following the ASTM D3039 standard procedure [17]. Prior to testing, the ends of the tensile coupons were sand blasted and end-tabbed with standard, 2.4 mm thick, glass-reinforced-plastic tabs. Strain gauges with a gauge resistance of 350 ± 1.0 Ω and of gauge factor of 2.03 were attached to the middle of the gauge section for each coupon. All specimens were strained using a 20 kN screwdriven Hounsfield mechanical tester at a strain rate of approximately 0.0005 min^{-1}. In general, transverse cracks were formed at composite strains higher than 0.2%. In all cases, measurements were made within a specified length of the coupon (Raman 'window') at applied strains required for transverse crack formation. To avoid unstable crack growth during Raman data acquisition all measurements were made by unloading the specimens to (a) 0.2% applied strain (which is below the crack initiation threshold value) and then (b) 0% applied strain.

2.4. Optical microscopy

Optical microscopic study was carried out on an Olympus microscope in order to measure the position of Kevlar® fibre from the ply interface. Sections of the specimen used for Raman measurements were cut parallel to the 90° ply cracks and embedded in resin to prepare for polishing. After polishing, the distance of the Kevlar® fibre from the ply interface was measured using optical microscopy and an Optomax V image analyser.

3. Results and discussion

3.1. Calibration of the Kevlar 49® fibre sensor

The basis of the laser Raman sensing technique, as mentioned earlier, is the stress or strain dependence of the Raman vibrational frequencies of almost all reinforcing fibres. The embedded Kevlar® fibre Raman sensor was calibrated by loading single filaments in air, plotting the shift of Raman wavenumber as a function of axial strain, and fitting the data with a least-squares-fit straight line (Fig. 3), giving $-4.38\,cm^{-1}\,\%^{-1}$ with respect to applied strain.

3.2. Local strains in the 0° plies as a result of transverse cracking

The strain, as a function of distance along a 25 mm long window of the Kevlar® fibre is shown in Fig. 4. The specimen was first strained to 0.23% and two cracks, identified as A and B in Fig. 4, appeared. To prevent the growth of additional cracks during the Raman observations, the specimen was relaxed to 0.2% applied strain and the measurements shown were then taken. The results of Fig. 4 show clear strain

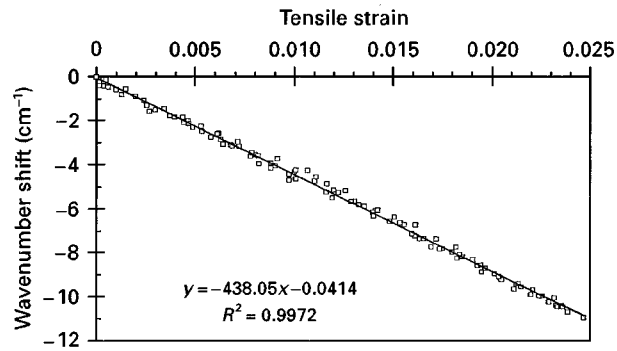

Figure 3 Raman wavenumber shift as a function of tensile strain for the Kevlar 49® fibres in air. This curve is used as a calibration curve for the conversion of the Raman frequency values into values of fibre strain in the composites.

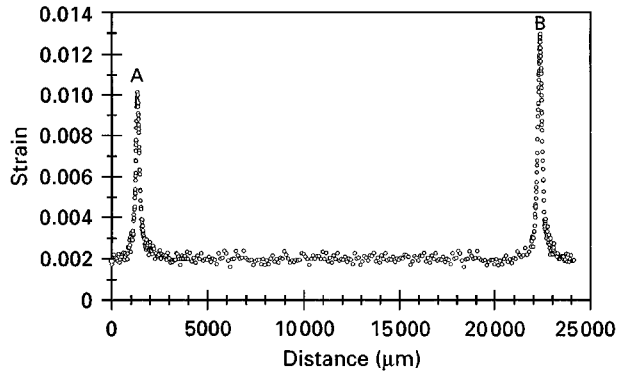

Figure 4 Strain distribution in the embedded Kevlar 49® fibre sensor as a function of distance over a 25 mm gauge length. Two transverse ply cracks, A and B, are present.

magnifications on the crack plane of approximately 5 and 6.5 times for cracks A and B, respectively. The differences in the two values are attributed to variations in the position of the fibre from the ply interface or, in other words, from the edge of the transverse ply crack. In general, it is expected that the strain magnification due to the crack has its maximum value at the ply interface and then decays with distance from the interface.

With increasing strain, more transverse cracks grew between A and B until a reasonably high crack density was achieved. The cracks were identified alphabetically as they appeared and the applied strains at which they appeared are indicated in Table I. The strain magnification was measured at an applied strain of 0.2% each time a new transverse crack appeared. The values of strain magnification as a function of position from the ply interface (measured by sectioning the coupons followed by optical microscopy and image analysis) are given in Fig. 5. The strain magnification decays from a value of about 6 at a distance of 10 μm from the interface to a value of about 2.5 at a distance of about 25 μm from the interface. If a straight line is fitted to the data (Fig. 5), a value of 8.3 is estimated as the maximum strain magnification at the ply interface, although it is unlikely that a linear relationship would obtain to the interface itself. In addition, by extrapolation it can be estimated that at a distance of approximately 40 μm from the interface, the 0° plies experience no strain magnification.

TABLE I Applied strain for which the cracks labelled A to H in Fig. 8 were first observed

Crack label	Applied strain (%)
A	0.0021
B	0.0023
C	0.0024
D	0.0027
E	0.0029
F	0.0032
G	0.0033
H	0.0035
I	0.0037
J	0.0040
K	0.0043

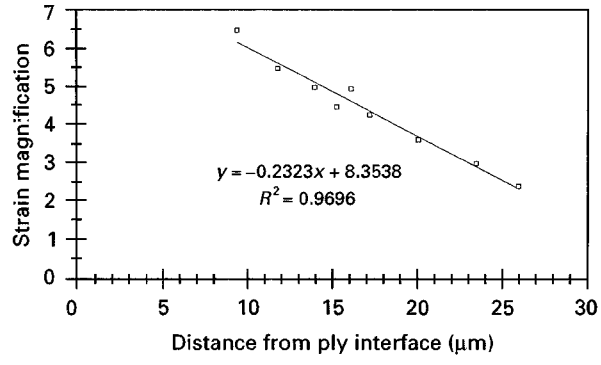

Figure 5 Strain magnification as a function of distance from the 0/90 interface for various transverse ply cracks. The solid line is a least-squares-fit to the experimental data.

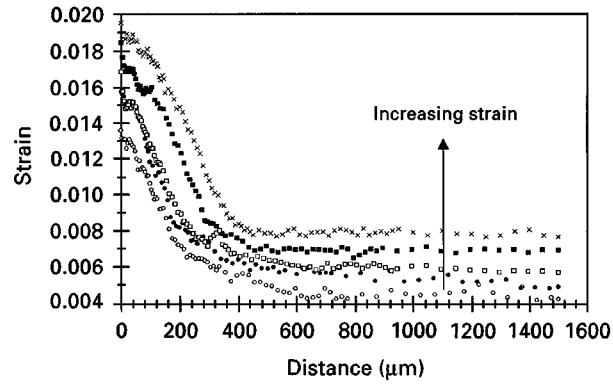

Figure 6 Strain distribution in the embedded Kevlar 49® fibre sensor as a function of distance from centre of a transverse crack (0 μm) for various levels of increasing applied strain.

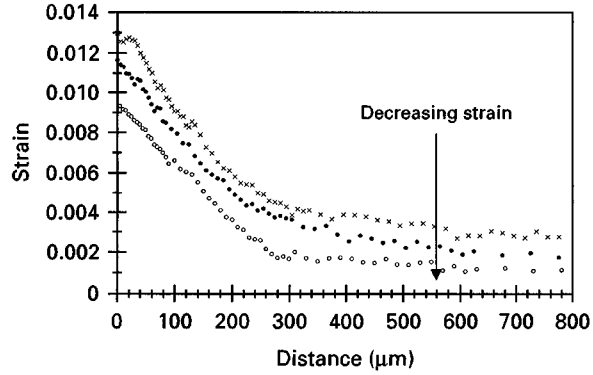

Figure 7 Strain distribution in the embedded Kevlar 49® fibre sensor as a function of distance from centre of a transverse crack (position = 0) for various levels of decreasing applied strain.

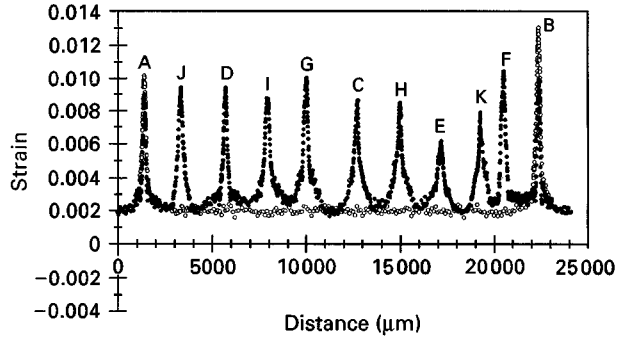

Figure 8 Strain distribution in the embedded Kevlar 49® fibre sensor within the 25 mm gauge length for a high crack density, showing 11 cracks, labelled A to K.

A number of effects suggest some matrix yielding and/or crack blunting occurs in the composites with increasing strain or with cycling which lead to changes in the strain profiles at the cracks. First, Figs 6 and 7 show how the strain magnification varies with increasing (Fig. 6) and decreasing (Fig. 7) applied strain for two different cracks (for simplicity, only half of the strain magnification profiles are shown). In both cases, a slight reduction in strain magnification is found at the higher applied strains and minor changes in the overall shape of the strain distributions are observed. Secondly, Fig. 8 shows the profile of cracks A and

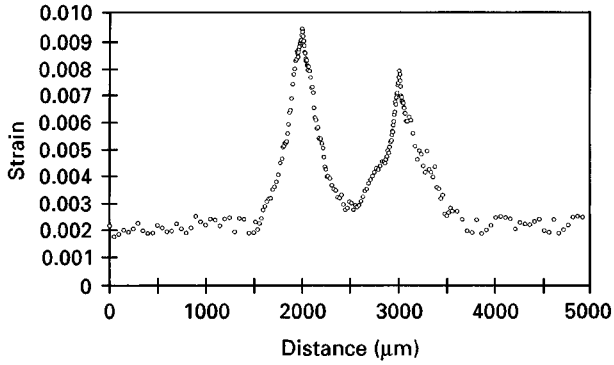

Figure 9 Strain distribution in the embedded Kevlar 49® fibre sensor for two closely spaced transverse ply cracks.

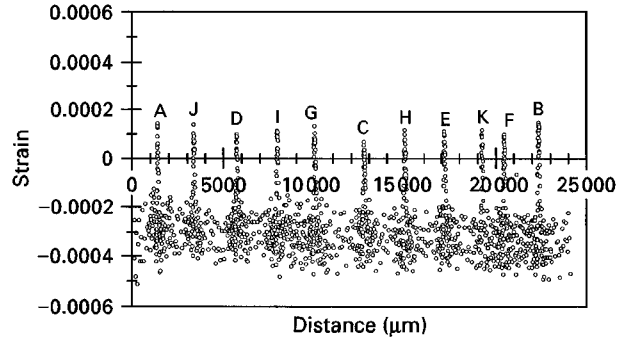

Figure 10 Strain distribution in the embedded Kevlar 49® fibre for the 11 cracks of Fig. 8 but at zero applied load. Note the peaks in the strain distribution at the crack planes.

B both before and after the appearance of cracks C to K. The maximum strain magnification observed for crack B is reduced somewhat which may be the consequence of matrix yielding and/or crack blunting as a result of cycling the specimen nine times during the development of cracks C to K.

The strain profiles also demonstrate crack interactions. For example, Fig. 9 shows the interaction of two cracks which are 0.8 transverse ply thicknesses apart. When the cracks interact due to their proximity, as in this case, the strain between the cracks does not return to its far field value. This contrasts with the results shown in Fig. 4, for which the cracks are so far apart that the far field strain is recovered. The high density, and variable spacing, of cracks in Fig. 8 enables an estimate of the crack interaction distance to be made. Crack interaction can be seen clearly when cracks are closer than 2 transverse ply thicknesses apart. This is in agreement with previous work based on changes in specimen compliance [2].

In Fig. 10 the strain distribution for no applied load is shown for the crack distribution of Fig. 8. As mentioned earlier, the fibre is in a state of compression due to the balanced longitudinal stresses in the 0° and 90° plies (compression in the 0° plies, tension in the 90° plies). The Raman results suggest a thermal strain in the 0° plies of about $-0.03\% \pm 0.01\%$, which is lower than a one-dimensional prediction of the thermal strain would suggest (about -0.07%) [18]. Part of this discrepancy can be attributed to the small strain applied to the Kevlar® fibre during the alignment of the fibre and the manufacture of the composite. The existence of this strain is indicated by the peaks in the strain profile in the plane of the matrix cracks at zero applied load. Fig. 10 shows that strains of up to $+0.015\%$ are found in the crack plane at zero applied load, whereas it would be expected that in the crack plane the strain should be zero since the balanced thermal stresses between the 0° and 90° plies are zero here. The remaining discrepancy may be attributable to the mismatch in thermal expansion coefficients between the Kevlar® fibre and the glass-reinforced epoxy resin into which it has been embedded. An important consequence of the peaks in the strain profile at zero applied load is that the location of the transverse cracks is defined quite accurately by these peaks. This allows accurate measurements of the residual strain of the cross-ply composite as a function of crack density [19].

4. Conclusions

Aramid fibre strain sensors have been embedded at one interface of 0°/90°/0° glass fibre composites. This has enabled the strain profile in the 0° plies resulting from matrix cracking in the 90° ply to be measured. Both the strain magnification in the vicinity of a crack, and crack interaction, can be monitored in this way. A maximum strain magnification of about 6 was measured at a distance of 10 μm from the ply interface and it is estimated that the strain magnification extends over a distance of about 40 μm from the interface into the 0° ply. Crack interactions are seen to occur when the cracks are less than about two transverse ply thicknesses apart. The existence of a small residual compressive strain in the 0° plies is clearly indicated by the results, but its precise measurement is complicated by the small pretensioning of the Kevlar® fibre during manufacture.

Acknowledgements

The assistance of members of the Raman Group of QMW is acknowledged, and particularly Mr A. Paipetis and V. Chohan.

References

1. A. PARVIZI, K. W. GARRETT and J. E. BAILEY, *J. Mater. Sci.* **13** (1978) 195.
2. L. BONIFACE, S. L. OGIN and P. A. SMITH, *Proc. R. Soc. Lond. A* **432** (1991) 427.
3. A. L. HIGHSMITH and K. L. REIFSNIDER, ASTM STP 775 (edited by K. Reifsnider) (1982) pp. 103–117.
4. P. A. SMITH and J. R. WOOD, *Compos. Sci. Technol.* **38** (1990) 85.
5. L. BONIFACE, S. L. OGIN and P. A. SMITH, ASTM STP **1156** (edited by W.W. Stinchcomb and N.E. Ashbaugh) (1993) pp. 139–160.
6. F. BASSAM, L. BONIFACE and S. L. OGIN, Proceedings of the Third International Conference on Deformation and Fracture of Composites, Guildford, UK, 1995, pp. 588–595.
7. M. CASLINI, C. ZANOTTI and T. K. O'BRIEN, *J. Compos. Technol. Res.* **9** (1987) 121.
8. N. LAWS and G. J. DVORAK, *J. Compos. Mater.* **22** (1988) 900.
9. L. N. McCARTNEY, S. HANNABY and P. M. COOPER, Proceedings of the Third International Conference on Deformation and Fracture of Composites, Guildford, UK, 1995, pp. 56–65.

10. J. A. NAIRN, *J. Compos. Mater.* **23** (1989) 1106.
11. F. J. GUILD, S. L. OGIN and P. A. SMITH, *ibid.* **27** (1993) 664.
12. L. SCHADLER and C. GALIOTIS, *Int. Mater. Rev.* **40** (1995) 116.
13. C. GALIOTIS, *Compos. Sci. Technol.* **42** (1991) 125.
14. B. ARJYAL and C. GALIOTIS, *Adv. Comp. Let.* **4/2** (1995) 47.
15. A. PAIPETIS, C. VLATTAS and C. GALIOTIS, *J. Raman Spectrosc.* **27** (1996) 519.
16. C. VLATTAS and C. GALIOTIS, *Polymer* **35/11** (1994) 2335.
17. American Society for Testing and Materials, Designation D3039-76 (Reapproved 1989), Standard Test Method for Tensile Properties of Fiber-Resin Composites, (ASTM, Philadelphia) pp. 118–122.
18. F. R. JONES and M. MULHERON, *Composites* **14** (1983) 281.
19. B. ARJYAL, C. GALIOTIS and S. L. OGIN, to be published.

Received 10 October 1997
and accepted 13 February 1998